Moments and Distribution Functions of the End-to-End Distance of Short Poly(dimethylsiloxane) and Poly(oxyethylene) Chains. Application to the Study of Elasticity in Model Networks

Miguel A. Llorente and Ana M. Rubio

Departamento de Quimica General y Macromoléculas, Facultad de Ciencias, Universidad Nacional de Educacion a Distancia (UNED), 28040 Madrid, Spain

Juan J. Freire*

Departamento de Quimica Fisica, Facultad de Ciencias Quimicas, Universidad Complutense, 28040 Madrid, Spain. *Received November 28, 1983*

ABSTRACT: High even moments and distribution functions of the end-to-end distance of short poly(dimethylsiloxane) (PDMS) and poly(oxyethylene) (POE) chains, described by means of the rotational isomeric state model, are evaluated according to a method recently proposed by Fixman et al. The application of the method to these heterogeneous chains includes a slight modification of the iterative procedure previously used for calculations of polymethylene (PM) moments. The distribution functions obtained this way are in good agreement with Monte Carlo calculations. The distribution functions of PDMS chains have been employed to derive an elastic equation that describes the non-Gaussian behavior of networks at high elongations. The method has been applied to model bimodal PDMS networks yielding a fair description of the experimental data. A semiquantitative estimation of the distribution of strains within the network chains indicates the expected high degree of nonaffineness in the deformation of these bimodal networks.

Introduction

The distribution of the end-to-end vector of a linear flexible chain, $F(\mathbf{R})$, and the simpler distribution of the end-to-end distance, $F(R)$, are functions of great theoretical importance, since they are related with many physical properties.[1,2] However, these functions cannot be obtained easily for realistic representations of short polymers. In recent years, the realistic rotational isomeric state model has been adopted to the calculation of $F(\mathbf{R})$ for a few types of chains such as polymethylenes[3,4] (PM), poly(dimethylsiloxane)[5] (PDMS), and polypeptides[6] by means of the Hermite series expansion procedure developed by Flory and Yoon,[3] but the results are not in good agreement with Monte Carlo calculations for the shortest chains due to the poor convergence of the series. A more accurate method, based on the use of a spherical harmonic representation of rotational operators to the evaluation of high moments together with a least-squares inference method to obtain the distribution function from these moments, has been proposed by Fixman et al.[7-9] and applied to the calculation of $F(R)$[9] and $F(\mathbf{R})$[10] for the simple polymethylene chain. The values of $F(R)$ obtained this way have been shown to be practically coincident with the Monte Carlo results[9] for chains with a number of bonds as low as $N = 10$. A fair agreement has also been observed with Monte Carlo functions computed[11] for $F(\mathbf{R})$.

In the present work we use this method to calculate $F(R)$ for PDMS and poly(oxyethylene) (POE). In contrast to PM, these "heterogeneous" chains have several different bond lengths, bond angles, or sets of statistical weights for the rotational angles included in every repeat unit.[5,12] Nevertheless, they can be appropriately described by means of sets of three symmetric rotational angles so that they can be treated with the theoretical scheme developed for PM, when some minor modifications are introduced. The extension of the method to asymmetric chains with an arbitrary number of rotational isomers together with the calculations of the asymmetric part of $F(\mathbf{R})$ for PDMS and POE are being currently tackled and will be reported soon.

Also in this work, we apply our theoretical results for $F(R)$ to a practical problem of current interest: the description of the non-Gaussian behavior in the elasticity of model networks. The Gaussian theory of rubber elasticity makes use of the Gaussian distribution function to describe the end-to-end distance of the network chains. In simple elongation the magnitude of interest is the "reduced force" defined as[13]

$$[f^*] = (f/A^*)/(\alpha - \alpha^{-2}) \tag{1}$$

where f is the elastic force at the equilibrium, A^* is the cross-sectional area of the unstretched sample, and α is the elongation ratio ($\alpha = L/L_0$). The simplest theory predicts that the reduced force is constant and independent of α. However, the experimental fact is that $[f^*]$ decreases as the elongation ratio increases. Thus, the results are usually represented by the semiempirical Mooney–Rivlin equation

$$[f^*] = 2C_1 + 2C_2\alpha^{-1} \tag{2}$$

where $2C_1$ and $2C_2$ are constants independent of α[14,15] with $2C_2$ being a measure of how the deformation changes from the affine to the phantom limit. This equation has been used extensively to describe the behavior of many elastomers at low and moderate elongations but fails at very high elongations where an upturn on the reduced force takes place, due to maximum chain extensibility. This non-Gaussian behavior has been usually described by introducing a more realistic form of the distribution function which takes into account that finite extensibility of the chain.[14] The treatment involves the use of the Langevin function and it has been applied to natural rubber by Mullins[16] and Morris.[17] However, natural rubber is not a good system to check these types of theories due to problems arising from stress-induced crystallinity which is also developed at high elongations. Moreover, the values obtained for the equivalent random link are too high.[14]

More recently, other alternative methods have been proposed. Gee[18] has deduced an empirical equation based on a power series expansion of the stored energy function with a restricted choice of the number of terms. A new term is added this way to the Mooney–Rivlin equation which takes into account the upturn at high elongations. This equation has been also applied to natural rubber using data taken from the references.

In the past few years Mark and co-workers[19,20] have published a series of data obtained on model networks of PDMS prepared by endlinking chains of two different

0024-9297/84/2217-2307$01.50/0

molecular weights. The resulting bimodal networks show non-Gaussian behavior due to maximum chain extensibility and are free from stress-induced crystallization.[19] These systems seem to be suitable to check any theory based on non-Gaussian statistics, although there will be some difficulties due to the bimodal character of the chains. The data for these networks have been analyzed by Kilian[21] by a method based on the van der Waals equation of state. Also, a treatment similar to that of Morris using the Langevin function has been tested and does not give good results since the values obtained for the number of equivalent random links are meaningless.[22]

In this paper we deduce an equation for the elastic force using the realistic end-to-end distribution functions corresponding to the rotational isomeric model mentioned above which shows the non-Gaussian behavior at high extension and we apply it to the data obtained by Mark and co-workers for PDMS bimodal networks.

Moments and End-to-End Distance Distribution Functions

Modification in the Theoretical Scheme. The procedures detailed in ref 8 (FS) and 9 (FF) for the calculation of moments and distribution functions of PM should be slightly modified in order to apply them to heterogeneous chains. Though changes affect mainly programing aspects we think that a few theoretical and technical remarks might be useful. As we will restrict the description to chains with three symmetric rotamers we will maintain the notation and symbols used in FS and FF. Equations 3.1 and 3.9 of ref 8, together with FF 2.13–2.16, give

$$C_{lm}(k) = (2\pi^{1/2})i^{-l}Z_N^{-1}\langle l,m \times (0|f_N(\mathbf{b}_N)\mathbf{R}_z(\varphi_N)\mathbf{R}_y(\theta_{N-1})\mathbf{U}_{N-1}{}^c f_{N-1}(\mathbf{b}_N) \ldots f_2(\mathbf{b}_N)\mathbf{R}_z(\varphi_2)\mathbf{R}_y(\theta_1)\mathbf{U}_1{}^c f_1(\mathbf{b}_N)|0\} \quad (3)$$

where $\mathbf{R}_z(\varphi_i)$ represents the diagonal matrix whose non-null elements are the rotational operators $R_z(\varphi_i)$ associated with the three different rotational isomers. The terms C_{lm} and their powers allow us to obtain the generalized moments $M_{lm}{}^{(k)}$ from which $F(\mathbf{R})$ is inferred.[9,10] In eq 3 we have reversed the order of the chain elements with respect to that established in eq FF 2.10 so that C_{lm} can be calculated for different values of N through an iterative procedure in the case of polymers with repeat units. Consequently, the statistical weight matrix $\mathbf{U}_i{}^c(\varphi_{i+1},\varphi_i)$ contains the first-order interaction parameter σ_i and the second-order interaction parameters ω_{i+1} and ψ_{i+1} for heterogeneous chains, so that, in the general case, this matrix is not coincident with Flory's standard matrix $\mathbf{U}_i(\varphi_i,\varphi_{i-1})$ containing all the parameters denoted by subscript i. Another implication is that now vector $\mathbf{k}$ and also the generalized moments are referred to a frame defined by bond vectors $\mathbf{b}_N$ and $\mathbf{b}_{N-1}$. Then the distribution function $F(\mathbf{R})$ with $\mathbf{R}$ referred to the first bonds $\mathbf{b}_1$ and $\mathbf{b}_2$ can only be calculated if the sequences of parameters associated with each repeat unit are introduced in an appropriately reversed order. Explicitly, for a repeat unit composed by n units we should perform the following substitutions of bond lengths, bond angles, rotational angles, and statistical weights written according to Flory's notation:[1]

$$b_i \leftrightarrow b_{n-i+1}$$
$$\theta_i \leftrightarrow \theta_{n-i}$$
$$\varphi_i \leftrightarrow \varphi_{n-i+1}$$
$$\sigma_i,\ \omega_i,\ \psi_i \leftrightarrow \sigma_{n-i+1},\ \omega_{n-i+2},\ \psi_{n-i+2} \quad (4)$$

(These substitutions with $n = N$ yield the initial ordering of chain elements specified in FF.) For the calculation of the symmetric C_{00} the orientation of $\mathbf{k}$ with respect to the reference frame is irrelevant and, consequently, the substitutions of parameters are unnecessary. This simplification was used through this work since C_{00} and its powers determine the high even moments $M_{00}{}^{2k}$ or $\langle R^{2p}\rangle$ from which the orientationally symmetric $F(R)$ is inferred. Moreover, the symmetric order of molecular parameters within the repeat units in the PDMS and POE chains allows one to avoid the substitutions even for the calculation of generalized moments with $l \neq 0$, if the chains contain N_r complete repeat units, i.e., if $N = 2N_r$ for PDMS or $N = 3N_r$ for POE.

Once a convenient ordering for the parameter sequences is assigned in each case, the iterative method described in FS can be applied by using the following modified versions of eq FS 3.2, 3.5, and 3.6:

$$E_N{}^{(p)}(l,m) = \sum_{q,l'}(-1)^m\binom{p}{q}(b_N)^{p-q}(z^{p-q})_m{}^{ll'} \times \sum_{m'=0}^{l'} P_{m,m'}{}^{(l')}(\theta_{N-1})[E_{N-1}{}^{(q)}(l',m') + 2\sigma_{N-1}R_{N-1}{}^{(q)}(l',m')] \quad (5)$$

$$R_N{}^{(p)}(l,m) = \sum_{q,l'}(-1)^m\binom{p}{q}(b_N)^{p-q}(z^{p-q})_m{}^{ll'} \times \{\cos(m\gamma_N)\sum_{m'=0}^{l'} P_{m,m'}{}^{(l')}(\theta_{N-1})[E_{N-1}{}^{(q)}(l',m') + \sigma_{N-1}(\psi_N + \omega_N)R_{N-1}{}^{(q)}(l',m')] + \sin(m\gamma_N)\sum_{m'=0}^{l'} Q_{m,m'}{}^{(l')}(\theta_{N-1})[\sigma_{N-1}(\psi_N - \omega_N)I_{N-1}{}^{(q)}(l',m')]\} \quad (6)$$

$$I_N{}^{(p)}(l,m) = \sum_{q,l'}(-1)^m\binom{p}{q}(b_N)^{p-q}(z^{p-q})_m{}^{ll'}\{\cos(m\gamma_N) \times \sum_{m'=0}^{l'} Q_{m,m'}{}^{(l')}(\theta_{N-1})[\sigma_{N-1}(\psi_N - \omega_N)I_{N-1}{}^{(q)}(l',m')] - \sin(m\gamma_N)\sum_{m'=0}^{l'} P_{m,m'}{}^{(l')}(\theta_{N-1})[E_{N-1}{}^{(q)}(l',m') + \sigma_{N-1}(\psi_N + \omega_N)R_{N-1}{}^{(q)}(l',m')]\} \quad (7)$$

In these equations γ_i represents the g^+ rotamer choice for φ_i. The terms $P_{m,m}{}^{(l')}(\theta_i)$ and $Q_{m,m}{}^{(l')}(\theta_i)$ are defined from eq FS 3.4 and 3.6 now in terms of the bond angle supplement θ_i specifically associated with the current iterative step. From the practical point of view it should be remarked that these elements are calculated and stored for the different possible values of θ_i before the iteration procedure starts. In consequence, the presence of several bond angle values does not represent a significant increase of the computation time. Though the storage needed for these terms is multiplied by the number of different angles, the total storage required for the calculations does not increase much, since it is mainly devoted to save the terms $(z^{p-q})_m{}^{ll'}$. Moreover, the particular values of bond lengths are taken into account by means of the constant factors $(b_i)^{p-q}$ in front of the $(z^{p-q})_m{}^{ll'}$ so that the final results are now obtained in real length units. Consequently, the global efficiency of the calculations in storage and time is similar to that achieved for homogeneous chains.[8,9]

The inference of $F(R)$ from its even moments $\langle R^{2p}\rangle$ is performed as described in FS section IV. Now the maximum value of R is taken to be $R_{max} = N\bar{b}$, where $\bar{b}$ is the root mean quadratic average length of a repeat unit

$$\bar{b} = (\sum_{i=1}^{n} b_i{}^2)^{1/2} \quad (8)$$

(We do not consider R_{max} to be the one associated to the "all-trans" conformation as we did for PM since this conformation does not correspond generally to the maximum extensibility of the chain.)

Results and Discussion

We have obtained values of the high even moments, $\langle R^{2p} \rangle$ and the end-to-end distance distribution function, $F(R)$, for PDMS and POE. We have not considered specifically the particular interactions of the terminal groups. For PDMS we have used the rotational isomeric state model parameters previously employed by Flory and Chang:[5] $b_{Si-O} = 1.64$ Å, $\theta_{Si-O-Si} = 37°$, $\theta_{O-Si-O} = 70°$, $\gamma_{Si-O} = \gamma_{O-Si} = 120°$ (for rotations on the Si–O and O–Si bond pairs), and statistical weights given by

$$U_{Si-O} = \begin{bmatrix} 1 & \sigma & \sigma \\ 1 & & 0 \\ 1 & & \sigma \end{bmatrix}$$

$$U_{O-Si} = \begin{bmatrix} 1 & & \sigma \\ 1 & & \sigma\omega \\ 1 & & \sigma \end{bmatrix}$$

with

$$\sigma = \exp(-8\ell/RT)$$

$$\omega = \exp(-1100/RT) \quad (9)$$

where RT is expressed in cal·mol^{-1}. We have performed our calculations with two temperature values: 25 and 110 °C.

For POE we have used the parameters proposed by Mark and Flory[12] ($b_{C-C} = 1.53$ Å, $b_{C-O} = 1.43$ Å, and $\theta = 70°$) for the three types of bond angles; $\gamma = 120°$ for the three types of internal rotations and statistical weights given by

$$U_{O-C} = \begin{bmatrix} 1 & \sigma & \sigma \\ 1 & \sigma & 0 \\ 1 & 0 & \sigma \end{bmatrix}$$

$$U_{C-C} = \begin{bmatrix} 1 & \sigma' & \sigma' \\ 1 & \sigma' & \sigma'\omega \\ 1 & \sigma'\omega & \sigma' \end{bmatrix}$$

and

$$U_{C-O} = \begin{bmatrix} 1 & \sigma & \sigma \\ 1 & \sigma & \sigma\omega \\ 1 & \sigma\omega & \sigma \end{bmatrix}$$

with

$$\sigma = \exp(-900/RT)$$

$$\sigma' = \exp(-430/RT)$$

$$\omega = \exp(-350/RT) \quad (10)$$

with RT in cal·mol^{-1}. We performed the calculations with $T = 60$ °C.

In Tables I and II we show the results obtained for the event moments for PDMS at $T = 110$ °C and POE at $T = 60$ °C. These results are coincident with the Monte Carlo values which we have also obtained according to the methods specified in ref 11 conveniently modified to take into account the existence of several different types of statistical weights for each polymer. In these Monte Carlo computations, we have used 8 or 12 statistical samples, each one including 50 000 independent conformations. Moreover, the characteristic ratios $C_N = \langle R^2 \rangle / N\bar{b}^2$ and the temperature coefficients, d ln $\langle R^2 \rangle$/dT are in agreement with previous independent calculations for PDMS[5] and POE.[12] All this serves as a numerical verification of the validity of our modified iterative procedure.

Table I
Even Moments $\langle R^{2p} \rangle$ in (Å)^{2p} for PDMS Chains of N Bonds at $T = 110$ °C[a]

	N		
p	10	20	40
1	1.218 092 2 (2)	2.935 273 8 (2)	6.403 896 2 (2)
2	1.574 590 0 (4)	1.046 901 0 (5)	5.772 755 2 (5)
3	2.124 082 8 (6)	4.125 652 3 (7)	6.245 465 4 (8)
4	2.963 041 6 (8)	1.735 731 8 (10)	7.576 724 4 (11)
5	4.248 115 1 (10)	7.660 282 9 (12)	9.955 626 1 (14)
6	6.231 206 9 (12)	3.508 881 2 (15)	1.388 737 9 (18)
7	9.318 594 9 (14)	1.656 493 8 (18)	2.030 554 2 (21)
8	1.416 934 7 (17)	8.019 387 1 (20)	3.085 275 6 (24)
9	2.185 953 9 (19)	3.966 605 0 (23)	4.841 296 4 (27)
10	3.415 756 8 (21)	1.998 905 3 (26)	7.809 104 2 (30)

[a] Power of ten that multiplies entries is in parentheses.

Table II
Even Moments $\langle R^{2p} \rangle$ in (Å)^{2p} for POE Chains of N Bonds at $T = 60$ °C

	N		
p	9	21	30
1	5.368 660 0 (1)	1.562 864 9 (2)	2.333 120 3 (2)
2	3.278 317 8 (3)	3.315 886 8 (4)	7.855 867 7 (4)
3	2.196 825 7 (5)	8.285 974 9 (6)	3.244 705 3 (7)
4	1.579 912 5 (7)	2.306 794 0 (9)	1.531 388 0 (10)
5	1.202 013 8 (9)	6.955 248 9 (11)	7.957 801 7 (12)
6	9.582 496 1 (10)	2.233 689 2 (14)	4.454 356 4 (15)
7	7.952 538 2 (12)	7.558 826 7 (16)	2.648 241 9 (18)
8	6.838 577 3 (14)	2.675 169 5 (19)	1.656 322 0 (21)
9	6.072 018 5 (16)	9.847 336 5 (21)	1.082 329 3 (24)
10	5.551 276 1 (18)	3.754 159 4 (24)	7.351 404 2 (26)

The inference of the end-to-end distribution function from its even moments leads to evaluating the coefficients g_k defined from

$$F(R) = P(R) \sum_{k=0}^{m} g_k R^{2k} \quad (11)$$

with

$$P(R) \propto \exp[-aR^2 - (bR^2)^s] \quad (12)$$

(We have set the maximum entropy value $s = 2$ through our calculations.) Convergence with m (the number of even moments employed in the procedure) has been reasonable enough in all cases so that we will restrict our comments to the distribution function results obtained for the highest value of m used in this work, $m = 10$. In Table III we present the values of the coefficients corresponding to PDMS chains of several values of N with $T = 25$ °C. These coefficients, and those corresponding to lower values of m, are involved in the calculations for network elasticity which will be described in the next section. The radial distributions

$$W(R) = 4\pi R^2 F(R) \quad (13)$$

are shown in Figures 1–3 for PDMS chains with $N = 10$, 20, and 40 at $T = 110$ °C and in Figures 4–6 for POE chains with $N = 9$, 21, and 30 at $T = 60$ °C. We have

Table III
Coefficients of Eq 11 for PDMS Chains of N Bonds at 25 °C Calculated with m = 10

	N				
g_i	20	30	50	80	200
0	5.541	1.697	1.107	1.038	1.019
1	−4.715 (1)	−2.857	−3.601 (−1)	−1.112 (−1)	−3.860 (−2)
2	1.916 (2)	2.329	5.565 (−1)	6.321 (−2)	1.038 (−2)
3	−4.179 (2)	2.647	−8.050 (−1)	−1.474 (−2)	2.101 (−3)
4	5.442 (2)	−8.047	6.073 (−1)	7.328 (−3)	−3.734 (−4)
5	−4.472 (2)	8.995	−1.731 (−1)	−1.135 (−3)	−3.154 (−5)
6	2.386 (2)	−5.453	1.814 (−3)	−3.393 (−4)	2.318 (−6)
7	−8.279 (1)	1.887	6.532 (−3)	4.319 (−5)	2.008 (−7)
8	1.807 (1)	−3.702 (−1)	−7.237 (−4)	4.892 (−6)	−1.961 (−9)
9	−2.250	3.818 (−2)	−2.933 (−5)	−3.210 (−7)	−3.924 (−10)
10	1.217 (−1)	−1.605 (−3)	5.154 (−6)	−2.618 (−8)	−7.076 (−12)

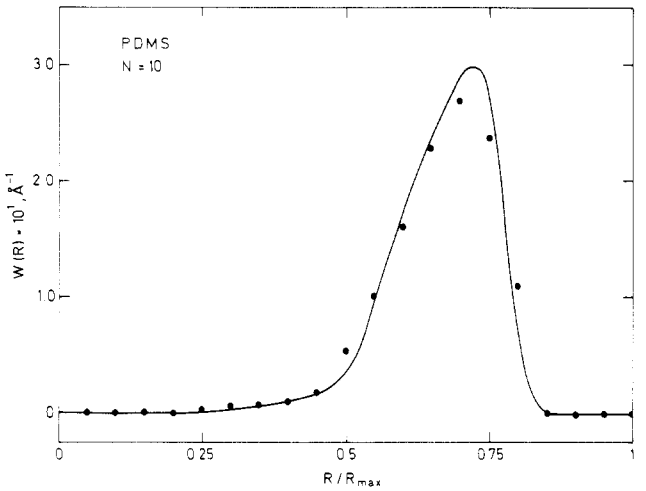

Figure 1. Inferred (solid line) and Monte Carlo (dots) values obtained in this work for the radial distribution, $W(R)$, vs. R/R_{max} for PDMS with N = 10 at T = 110 °C.

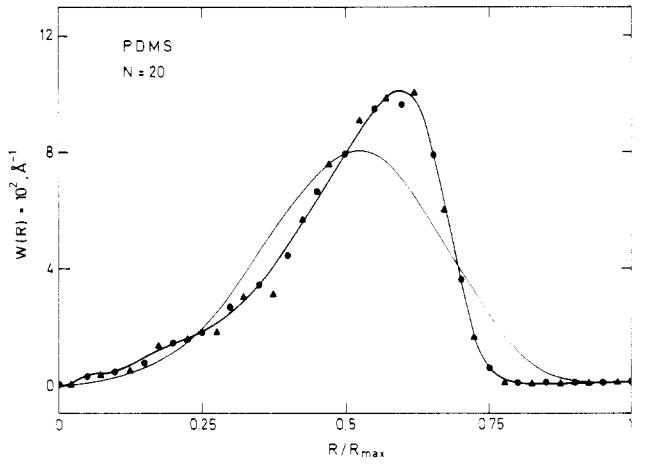

Figure 2. $W(R)$ vs. R/R_{max} as in Figure 1 but with N = 20. The Monte Carlo (▲) and Hermitian (thin line) results obtained by Flory and Chang[5] are also included.

compared our values for PDMS chains with N = 20 and 40 with those obtained by Flory and Chang[5] through both Monte Carlo calculations and the Hermite series expansion procedure. Our results are in much better accordance with the Monte Carlo results than the Hermitian values. In fact, both our results and the Monte Carlo distribution functions are practically coincident if the latter are shifted to the center of their statistical interval (as plotted in Figures 2 and 3) instead of being associated to the interval right limit, as they are apparently disposed in Figures 15 and 16 of ref 5.

Moreover, we have performed our own Monte Carlo calculations for $W(R)$ following the procedure described in ref 11 (conveniently modified for heterogeneous chains). The results obtained this way for PDMS and POE are

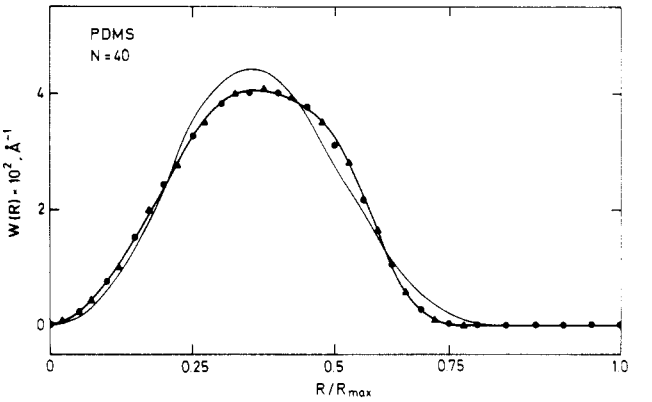

Figure 3. $W(R)$ vs. R/R_{max} as in Figure 2 but with N = 40.

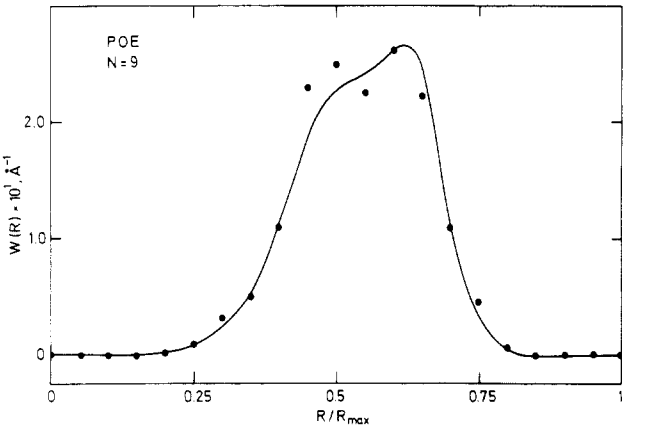

Figure 4. $W(R)$ vs. R/R_{max} for POE with N = 9 at T = 60 °C. Inferred (solid line) and Monte Carlo (dots) results obtained in this work are included.

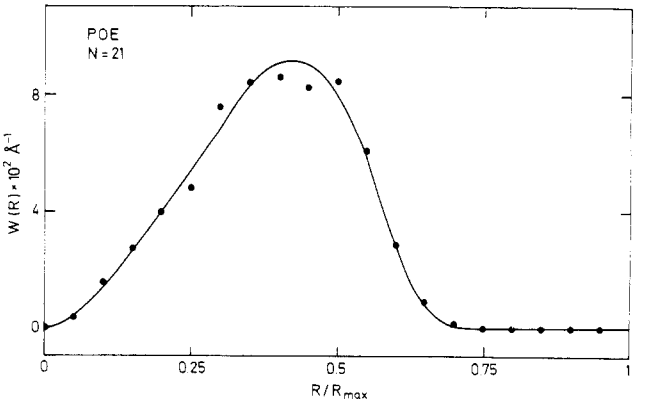

Figure 5. $W(R)$ vs. R/R_{max} as in Figure 4 but with N = 21.

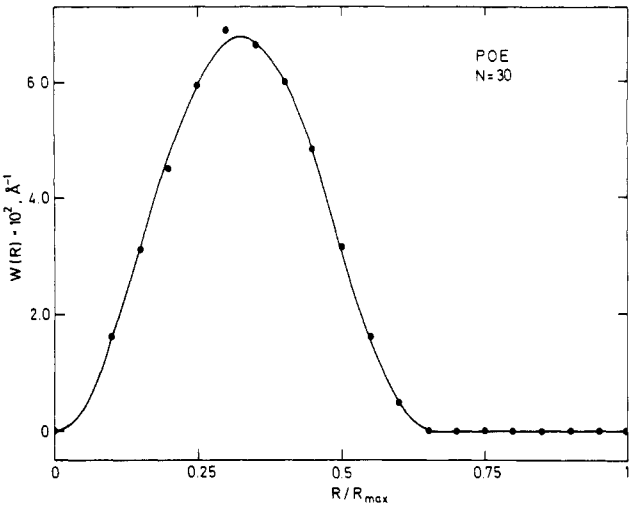

Figure 6. $W(R)$ vs. R/R_{max} as in Figure 4 but with $N = 30$.

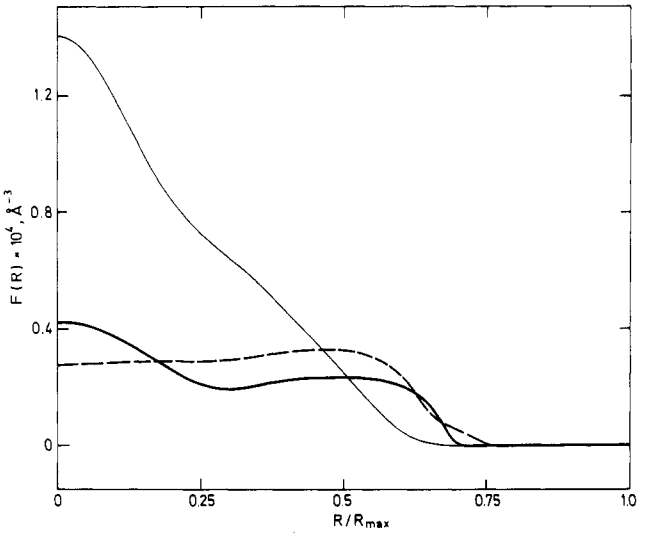

Figure 7. $F(R)$ vs. R/R_{max} for PM with $N = 20$ at $T = 140$ °C (– – –), PDMS with $N = 20$ at $T = 110$ °C (thick line), and POE with $N = 21$ at $T = 60$ °C (thin line).

included in Figures 1–5. For PDMS with $N = 20$, our Monte Carlo distribution functions are slightly smoother than the results obtained by Flory and Chang, as can be observed in Figure 2. The agreement between the Monte Carlo and the inferred results is good, though only wide statistical intervals are able to yield reasonably smooth Monte Carlo distribution functions for the shortest chains, $N = 9$ or 10. A further improvement in the comparison can easily be achieved by using still wider intervals in order to smooth the roughest regions of the Monte Carlo distribution functions since in these regions the inferred curve lies between the Monte Carlo points. It should also be remarked that we do not know of previous calculations for $W(R)$ in the case of the POE chains so that our Monte Carlo results are the only possible check for the values obtained by inference from the moments.

In Figure 7, we compare the shapes of $F(R)$ for PM[9] with $N = 20$ at $T = 140$ °C (considering $R_{max} = N\bar{b}$, as used through this work), PDMS with $N = 20$ at 110 °C and POE with $N = 21$ at 60 °C. It can be observed that the POE molecules are considerably more flexible than the other chains. PDMS and PM present similar stiffness, though the distribution function of PDMS is more irregular. The influence of temperature on these conclusions should be small.

Application to Rubber Elasticity

Derivation of the Elastic Equations. In order to obtain an elastic equation from the distribution function given by eq 11–13, the usual procedure is followed.[14,23] The free energy for a chain is given by

$$A = -k_B T \ln W(R) \tag{14}$$

where $W(R)$ is given by eq 13. The variation of this function at constant temperature is given in terms of the coefficients associated to the realistic distribution function, eq 11, by

$$\Delta A = -k_B T[\ln \sum_{k=0}^{m} g_k(\alpha_x^2 x^2 + \alpha_y^2 y^2 + \alpha_z^2 z^2)^k - \ln \sum_{k=0}^{m} g_k(x^2 + y^2 + z^2)^k] + k_B Ta[\alpha_x^2 x^2 + \alpha_y^2 y^2 + \alpha_z^2 z^2 - (x^2 + y^2 + z^2)] + k_B Tb^s[(\alpha_x^2 x^2 + \alpha_y^2 y^2 + \alpha_z^2 z^2)^s - (x^2 + y^2 + z^2)^s] \tag{15}$$

where α_x, α_y, and α_z are the deformations ($\alpha_i = L_i/L_{0,i}$) in the three directions x, y, and z, respectively. $k_B T$ is the Boltzmann factor, and L_i and $L_{0,i}$ are the lengths of the stretched and unstretched sample, respectively.

In simple elongation, for example along the x direction, one has a deformation defined by the following expansion factors:

$$\alpha_x = \alpha \tag{16}$$

$$\alpha_y = \alpha_z = \alpha^{-1/2} \tag{17}$$

noting that for the equilibrium state

$$\langle x^2 \rangle_0 = \langle y^2 \rangle_0 = \langle z^2 \rangle_0 = \langle R^2 \rangle / 3 \tag{18}$$

Equations 16 and 17 are valid assuming that the volume of the elastomer does not change with deformations. Equation 18 holds due to the isotropy of the material and because the cross-links do not change the chain dimensions. Therefore, for a network of N_T chains and in simple elongation, eq 15 becomes

$$\Delta A = -N_T k_B T[\ln \sum_{k=0}^{m} (g_k/3^k)(\alpha^2 + 2/\alpha)^k - \ln \sum_{k=0}^{m} g_k] + (N_T k_B Ta/3)(\alpha^2 + 2/\alpha - 3) + (N_T k_B Tb^s/3^s)[(\alpha^2 + 2/\alpha)^s - 3^s] \tag{19}$$

Then the elastic force can be obtained as

$$f = (\partial \Delta A/\partial L)_{T,V} = -(N_T k_B T/L_i)\left\{ \frac{\sum_{k=1}^{m} (k g_k/3^k)(\alpha^2 + 2/\alpha)^{k-1}(2\alpha - 2/\alpha^2)}{\sum_{k=0}^{m} (g_k/3^k)(\alpha^2 + 2/\alpha)^k} + (a/3)(2\alpha - 2/\alpha^2) + (b^s/3^s)s(\alpha^2 + 2/\alpha)^{s-1}(2\alpha - 2/\alpha^2) \right\} \tag{20}$$

Dividing by the cross-sectional area of the sample one can express the factor in front of the right side of eq 20 as a function of the molecular weight between cross-links (M_c) and the density (ρ) ($N_T k_B T/V = \rho RT/M_c$). The final expression for the elastic force per unit area is therefore

$$f^* = (2\rho RT/3M_c)(\alpha - \alpha^{-2})\left\{a + (2b^2/3) \times (\alpha^2 + 2/\alpha)\frac{\sum_{k=1}^{m} k g_k[(\alpha^2 + 2/\alpha)/3]^{k-1}}{\sum_{k=0}^{m} (g_k/3^k)(\alpha^2 + 2/\alpha)^k}\right\} \quad (21)$$

where the value $s = 2$ corresponding to maximum entropy has been taken. This expression is valid for an affine deformation and is represented in Figure 8 for three different numbers of units. In each case, the effect of the number of polynomial coefficients employed, $m + 1$, is shown. As expected, the influence of the number of these coefficients decreases with increasing length of the chains. As can be seen, eq 21 could be appropriate to describe the non-Gaussian behavior at high elongation since, in every case, it shows an upturn in the elastic force and, on the other hand, the deviation from the Gaussian behavior increases with decreasing length of the chains.

Usually the experimental data are reported by using the reduced stress by means of a Mooney–Rivlin plot; therefore, it is necessary to express the above treatment in a similar form. This can be done by introducing the front factor corresponding to the phantom limit $(1 - 2/\phi)$ (ϕ is the functionality of the junction points) and including the departure from this limit with a $2C_2$ term. Thus

$$[f^*] = 2C_1\left\{a + (2b^2/3) \times (\alpha^2 + 2/\alpha) - \frac{\sum_{k=1}^{m} k g_k[(\alpha^2 + 2/\alpha)/3]^{k-1}}{\sum_{k=0}^{m} (g_k/3^k)(\alpha^2 + 2/\alpha)^k}\right\} + 2C_2\alpha^{-1} \quad (22)$$

where

$$2C_1 = (2/3)v_{2c}^{2/3}(\rho RT/M_c)(1 - 2/\phi) = (\rho RT/3M_c)v_{2c}^{2/3} \qquad (\phi = 4) \quad (23)$$

The factor $v_{2c}^{2/3}$ is introduced to take into account the conditions in which the network was formed, v_{2c} being the volume fraction of the polymer during the cross-linking reaction.[24] Equation 22 can then be used to interpret the experimental data with only two parameters, the constants $2C_1$ and $2C_2$. The first one is related with the cross-links density through M_c and the second with the deviation from the phantom limit. As explained above, the introduction of the detailed molecular structure through the distribution functions makes it unnecessary to use any other parameter to describe the non-Gaussian nature of the chain.

Comparison with Experimental Data. Unfortunately, experimental data showing non-Gaussian behavior at high extensions and free from problems due to stress-induced crystallization are not available for unimodal networks. The only reliable data showing this effect are those of Mark et al.[19,20] on bimodal PDMS networks. In spite of this shortcoming, it seems to be worth trying to fit these results with eq 22, at least in a tentative way. A first option is to assume that the strain is distributed uniformly between short and long chains. Of course, this constitutes a rough approximation, but it may be indicative of the influence of non-Gaussian behavior at high elongations in the experimental curves. The comparison with every network sample is performed by using the theoretical constants a and b and the coefficients g_i relative to the number of units corresponding to the average molecular weight of the network chains. As Figure 8 shows, the number of polynomial coefficients used, m, is not very important except for very short chains, so that three coefficients have been used in all cases. The results are shown in Figures 9–11 and the numerical values are given in Table IV. As can be seen, the curves fit fairly well the experimental points in the cases of the systems with molecular weights 18 500 + 1100 and 18 500 + 660. For the system with very short chains (18 500 + 220) the agreement is poor. Columns 6 and 7 of Table IV give the values of the constants $2C_1$ and $2C_2$ obtained by the least-squares analysis of eq 22. The last column gives the molecular weights between cross-links obtained from the constant $2C_1$. The comparison of these values with those obtained from the average molecular weight of the samples used to prepare the networks, $\bar{M}_n$, indicates that the agreement

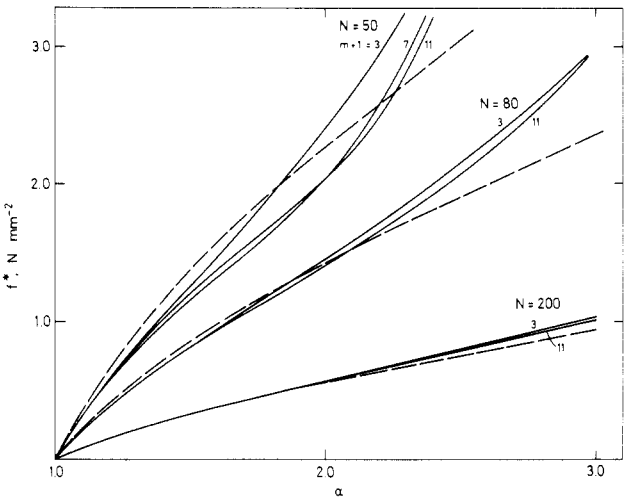

Figure 8. Plots of the elastic force given by eq 21 for chains of different length at 25 °C. The number of coefficients introduced in the calculations (see text) is also indicated. Dashed curves correspond to the Gaussian limit.

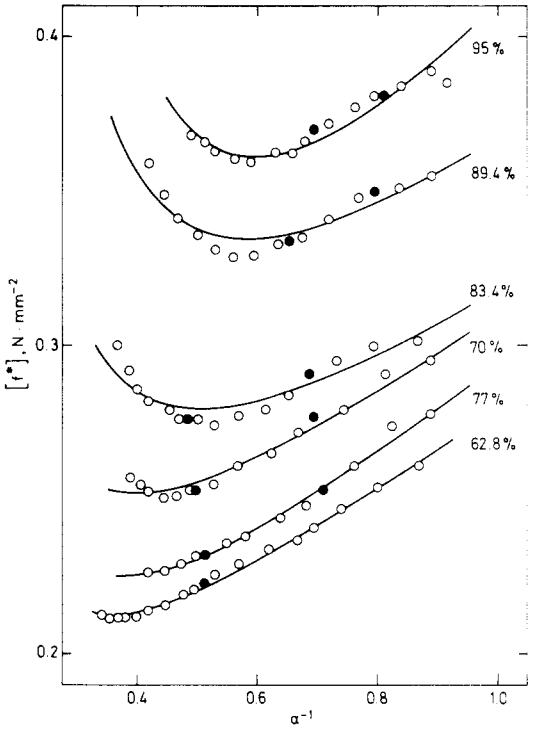

Figure 9. Experimental results[19] corresponding to the system 18 500 + 1100 molecular weights of different compositions fitted according to eq 22.

Table IV
Numerical Parameters Used and Results Obtained by Fitting the Data of Bimodal PDMS Networks

$10^{-3}M_s$[a]	% short chains	a	b	$10^{-3}\bar{M}_n$[b]	$2C_1$, N/mm^2	$2C_2$, N/mm^2	$10^{-3}M_c$[c]
1.10	95.0	0.845	0.468	1.97	0.174	0.188	4.45
	89.4	1.123	0.348	2.94	0.183	0.118	4.23
	83.4	1.238	0.286	4.00	0.149	0.109	5.20
	77.0	1.303	0.247	5.10	0.106	0.144	7.30
	70.0	1.335	0.224	6.30	0.128	0.127	6.05
	62.8	1.347	0.220	7.57	0.102	0.134	7.59
0.66	90.0	1.015	0.398	2.44	0.292	0.0145	2.65
	80.0	1.255	0.277	4.23	0.190	0.0942	4.07
	70.0	1.330	0.228	6.00	0.160	0.0946	4.84
	60.0	1.348	0.220	7.80	0.122	0.0989	6.35
0.22	90.0	0.873	0.459	2.05	0.376	−0.170	2.06
	85.0	1.124	0.349	2.96	0.291	−0.094	2.66
	75.0	1.286	0.257	4.79	0.211	0.0038	3.67
	60.0	1.348	0.220	7.80	0.148	0.0867	5.23

[a] Molecular weight of short chains (for long chains $M_l = 18.5 \times 10^3$). [b] Average value of M_s and M_l. [c] Molecular weight between cross-links obtained from the constant $2C_1$ (eq 23).

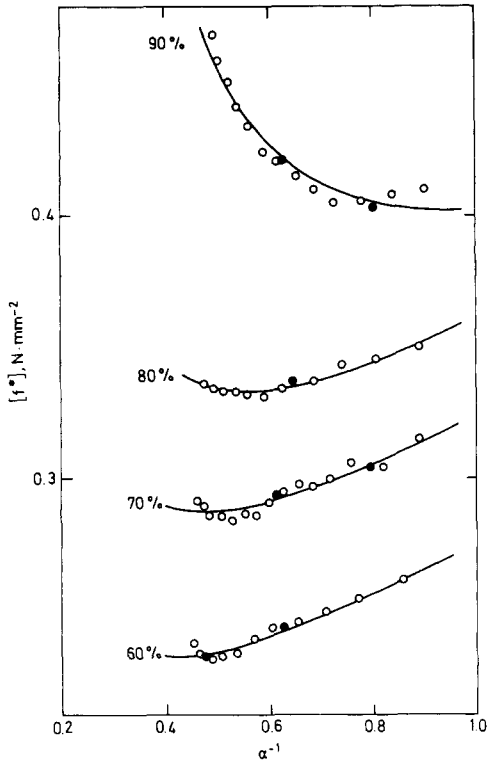

Figure 10. Experimental results[20] corresponding to the system 18 500 + 660 molecular weights fitted according to eq 22.

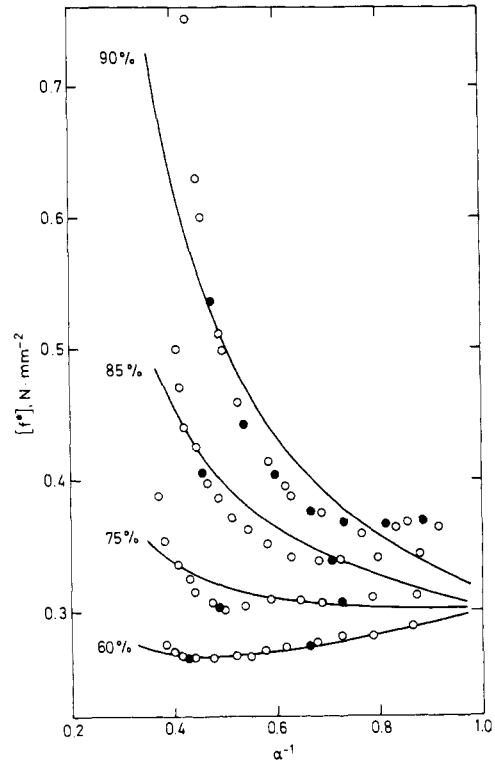

Figure 11. Experimental results[20] corresponding to the system 18 500 + 220 molecular weights fitted according to eq 22.

is fairly good. Though deviations occur in some cases, the agreement can be considered satisfactory in view of the lack of realism of the approximation above described, mainly manifested in the more pronounced upturns exhibit by the experimental data with respect to the theoretical curves.

In order to get a better understanding of how stresses and deformations are distributed within the chains, attempts were made to separate the contribution of the two kinds of chains. We assume that all the chains exert the same stress independently of their lengths so that junction points are at mechanical equilibrium in the stretched state. Therefore the total force is given by

$$f = N_T X_s f_s(\alpha_s) + N_T X_l f_l(\alpha_l) \tag{24}$$

with

$$f_l(\alpha_l) = f_s(\alpha_s) \tag{25}$$

where X_s and X_l are the number fractions of short and long chains, respectively, and $f_s(\alpha_s)$ and $f_l(\alpha_l)$ are the forces exerted by the short and long chains referred to their own deformations. Dividing eq 24 by the total volume, we have

$$f/L^0A = (\phi_l \rho RT/M_l L_l^0) f_l'(\alpha_l) + (\phi_s \rho RT/M_s L_s^0) f_s'(\alpha_s) \tag{26}$$

where $f_i' = f_i L_i^0/RT$. The volume fractions of short and long chains are

$$\phi_l V = X_l N_T M_l/\rho \tag{27}$$

$$\phi_s V = X_s N_T M_s/\rho \tag{28}$$

The force per unit area is then

$$\begin{aligned} f^* &= (\rho RT)(L^0/L_l^0) f_l'(\alpha_l)(\phi_l/M_l + \phi_s/M_s) \\ &= (\rho RT)(L^0/L_s^0) f_s'(\alpha_s)(\phi_l/M_l + \phi_s/M_s) \end{aligned} \tag{29}$$

and the ratio ϕ_i/M_i can be expressed by

$$\phi_i/M_i = X_i N_T/\rho V = X_i/\bar{M}_n \tag{30}$$

Table V
Chain Dimensions of PDMS at 25 °C

$\bar{M}_n$	N	C_N	$\langle r^2\rangle_N^{1/2}$, Å	α^{max}
18500	500	6.11	90.65	7.40
1100	29.7	5.55	21.06	1.89
660	17.8	5.26	15.87	1.50
220	6.0	3.71	7.74	1.04

where $\bar{M}_n$ is the average molecular weight of short and long chains. Finally, the elastic force per unit area is given by

$$f^* = (\rho RT)(L^0/L_l^0)M_n^{-1}f_l'(\alpha_l) = (\rho RT)(L^0/L_s^0)M_n^{-1}f_s'(\alpha_s) \quad (31)$$

In order to interpret the experimental results, the following procedure is used: First we discount the $2C_2$ term obtained in our previous fitting from the total force and express the ratios L_i^0/L^0 through the equilibrium chain dimension, $\langle r^2\rangle_i$

$$L_i^0/L^0 = \langle r^2\rangle_i^{1/2}/(X_l\langle r^2\rangle_l^{1/2} + X_s\langle r^2\rangle_s^{1/2}) \quad (32)$$

The long chains are represented by the Gaussian distribution function whereas for the short ones we use the distribution functions given by eq 11. Then we have

$$G = f^* - 2C_2(1 - \alpha^{-3}) = (\rho RTv_{2c}^{2/3}/2\bar{M}_n)(L^0/L_l^0) \times (\alpha_l - \alpha_l^{-2}) = (\rho RTv_{2c}^{2/3}/3\bar{M}_n)(L^0/L_s^0)f_s'(\alpha_s) \quad (33)$$

with

$$f'(\alpha_s) = (\alpha_s - \alpha_s^{-2})\{a + (2b^2/3)(\alpha_s^2 - 2/\alpha_s) - \{\sum_{k=1}^{m} kg_k[(\alpha_s^2 + 2/\alpha_s)/3]^{k-1}/\sum_{k=0}^{m}(g_k/3^k)(\alpha_s^2 + 2/\alpha_s)^k\}\} \quad (34)$$

For both types of chains we have introduced the factor $(1 - 2/\phi = 1/2)$ relative to phantom networks, and the factor $v_{2c}^{2/3}$ as done in eq 23.

We also need a relationship between the deformation of short and long chains and the macroscopic deformation. We take

$$\alpha = \phi_s^{1/3}\alpha_s + (1 - \phi_s^{1/3})\alpha_l \quad (35)$$

The different values of the chain dimensions were obtained from

$$\langle r^2\rangle_N = C_N N b^2 \quad (36)$$

in which the characteristic ratios C_N are values interpolated from our theoretical results for $\langle R^2\rangle/Nb^2$ for PDMS at $T = 25$ °C. These interpolated values are shown in Table V. (For $N = 500$ we have taken for C_N the estimated asymptotic value.) In every case the value of $2C_2$ given in Table IV is used in eq 33, and the values of α_s and α_l and the factor $2C_1' = \rho RTv_{2c}^{2/3}/\bar{M}_n$ were obtained by fitting simultaneously eq 33–35. Since we are dealing now with distribution functions of very short chains, 11 polynomial coefficients are used in eq 34; i.e., $m + 1 = 11$.

The results are shown in Figures 12 and 13. The maximum extensibility shown in these figures for the short chains, α_s^{max}, have been estimated by the method described in ref 19. The values of α_s^{max} are given in the last column of Table V. It can be seen that the long chains deform much more than the short ones, the latter approaching their limit very rapidly. In the system 660 + 18500 the data at low deformations are not conclusive since, as shown in Figure 14, the form of the theoretical curve f_s' vs. α_s for $N = 20$ is not sensitive to variations of α_s in the range of low values of this variable. The third system (220 + 18500)

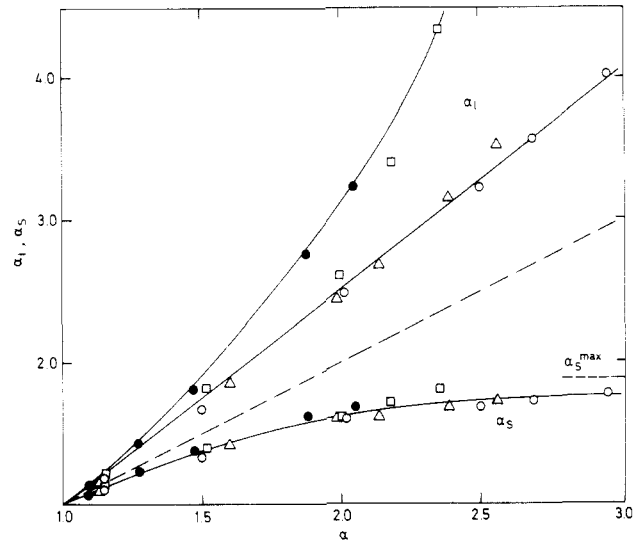

Figure 12. Deformations of long and short chains as a function of the macroscopic deformation for the system 18500 + 1100 molecular weights. Only representative points for each composition are plotted: (⊙) 62.8%, (△) 70%, (□) 83.4%, and (●) 95%. The dashed line corresponds to the affine deformation. The solid lines represent the approximate trends followed by the different sets of points.

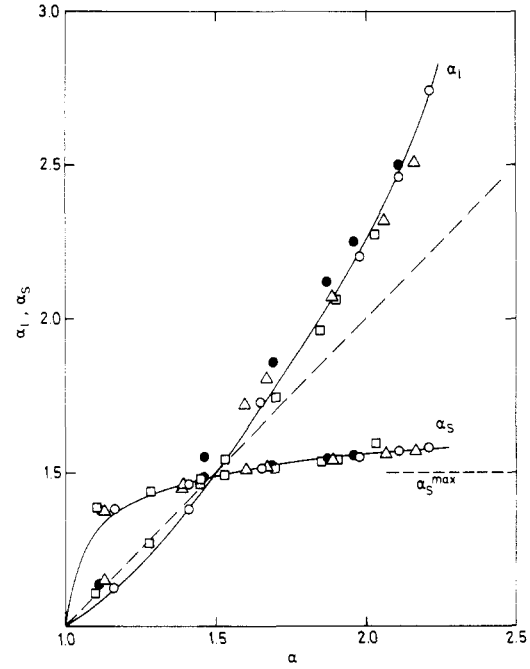

Figure 13. Deformations of long and short chains as a function of the macroscopic deformation, for the system 18500 + 660 molecular weights. Only representative points for each composition are plotted: (⊙) 60%, (△) 70%, (●) 80%, and (□) 90%. The dashed line corresponds to the affine deformation.

cannot be studied this way since for these very short chains the function $f_s'(\alpha_s)$ is negative for low values of α_s, due to the same lack of sensitivity.

We must point out that the values of the constant $2C_1'$ required to fit the experimental points are higher than those obtained by fitting eq 22, yielding molecular weights about half the values previously calculated. Consequently, the results corresponding to the separate contributions can be only considered from a qualitative point of view since the distribution of strains has been performed in an empirical way. Nevertheless, we think they are very illustrative of how the strains are distributed within the network chains, showing the high degree of nonaffineness in

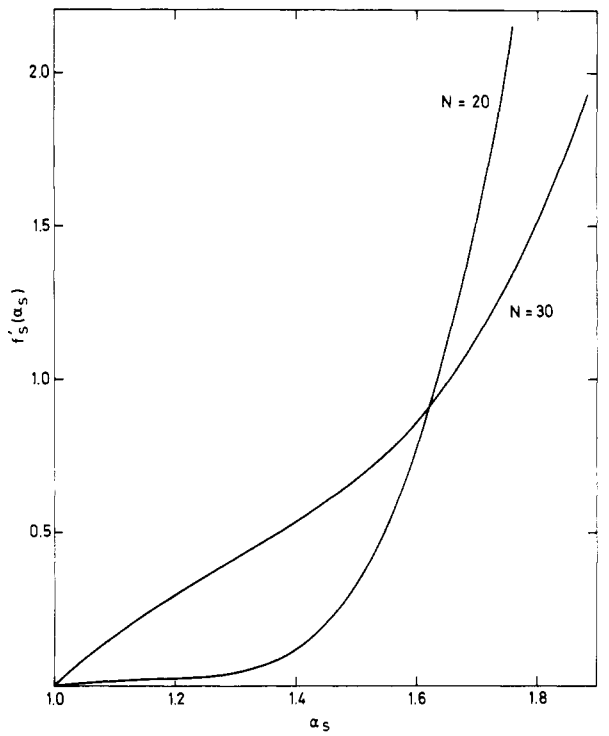

Figure 14. Plots of the function $f_s'(\alpha_s)$, given by eq 34, at 25 °C, using a number of coefficients $m + 1 = 11$, for two short chains of different number of repeat units.

the deformation of these bimodal networks.

After the results reported in this work were obtained, we became aware of the work on network elasticity performed very recently by Mark and Curro.[25-27] These authors obtained the elastic force curves by means of realistic distribution functions in a way similar to ours. Two main differences, however, exist between these descriptions. First, Mark and Curro calculated the distribution functions through a Monte Carlo method, the results being then curve fitted with the help of a least-squares numerical technique. Since our treatment is based on evaluating the functions by inference from their even moments, which are calculated using iterative formulas, it can be considered a significantly more efficient computational method which provides a similar degree of accuracy. Second, Mark and Curro consider affine deformation as an initial assumption and then perform a theoretical nonaffine partition between short and long chains based on the maximum entropy principle. Their preliminary curve trends are not totally satisfactory since the position of the upturn does not appreciably change with composition as it does in experimental curves. Perhaps this effect could be attributed to their partition procedure. On the other hand, our approach is substantially different in this respect since we have employed an empirical decomposition of α by direct comparison with the data.

Acknowledgment. A. M. Rubio gratefully acknowledges the award of a fellowship from the Ministerio de Educación y Ciencia (P.F.P.I.). This work was supported in part by Grant 0933/82 from the Comisión Asesora de Investigación Cientifica y Tēcnica.

Registry No. POE (SRU), 25322-68-3.

References and Notes

(1) Flory, P. J. "Statistical Mechanics of Chain Molecules"; Wiley: New York, 1969.
(2) Yamakawa, H. "Modern Theories of Polymer Solutions"; Harper and Row: New York, 1971.
(3) Flory, P. J.; Yoon, D. Y. *J. Chem. Phys.* **1974**, *61*, 5358.
(4) Yoon, D. Y.; Flory, P. J. *J. Chem. Phys.* **1974**, *61*, 5366.
(5) Flory, P. J.; Chang, V. W. C. *Macromolecules* **1976**, *9*, 33.
(6) Conrad, J. C.; Flory, P. J. *Macromolecules* **1976**, *9*, 41.
(7) Fixman, M. *J. Chem. Phys.* **1973**, *58*, 1559.
(8) Fixman, M.; Skolnick, J. *J. Chem. Phys.* **1976**, *65*, 1700.
(9) Freire, J. J.; Fixman, M. *J. Chem. Phys.* **1978**, *69*, 634.
(10) Freire, J. J.; Rodrigo, M. M. *J. Chem. Phys.* **1980**, *72*, 6376.
(11) Rubio, A. M.; Freire, J. J. *Macromolecules* **1982**, *15*, 1411.
(12) Mark, J. E.; Flory, P. J. *J. Am. Chem. Soc.* **1965**, *87*, 1415.
(13) Mark, J. E.; Sullivan, J. L. *J. Chem. Phys.* **1977**, *66*, 1006.
(14) Treloar, L. R. G. "The Physics of Rubber Elasticity", 3rd ed.; Clarendon Press: Oxford, 1975.
(15) Mooney, M. *J. Appl. Phys.* **1948**, *19*, 434. Rivlin, R. S. *Philos. Trans. R. Soc. London, Ser. A* **1948**, *241*, 379.
(16) Mullins, L. *J. Appl. Polym. Sci.* **1959**, *2*, 257.
(17) Morris, M. C. *J. Appl. Polym. Sci.* **1964**, *8*, 545.
(18) Gee, G. *Macromolecules* **1980**, *13*, 705.
(19) Andrady, A. L.; Llorente, M. A.; Mark, J. E. *J. Chem. Phys.* **1980**, *72*, 2282.
(20) Llorente, M. A.; Andrady, A. L.; Mark, J. E. *J. Polym. Sci., Polym. Phys. Ed.* **1981**, *19*, 621.
(21) Kilian, H. G. *Colloid Polym. Sci.* **1981**, *259*, 1151.
(22) Andrady, A. L.; Llorente, M. A.; Mark, J. E., unpublished results.
(23) Mark, J. E. *J. Chem. Educ.* **1981**, *58*, 898.
(24) Llorente, M. A.; Mark, J. E. *J. Chem. Phys.* **1979**, *71*, 682.
(25) Curro, J. G.; Mark, J. E. *Polym. Prepr., Am. Chem. Soc., Div. Polym. Chem.* **1983**, *24*, 210.
(26) Mark, J. E. 29th Symposium on Macromolecules. Communication IV.5, Bucharest, 1983, and private communication.
(27) Mark, J. E.; Curro, J. G. *J. Chem. Phys.* **1983**, *79*, 5705.